

# Accurate prediction of ground motion using an hp-adaptive discontinuous Galerkin finite-element method (DG-FEM)

V. Etienne<sup>1</sup>, E. Chaljub<sup>2</sup>, J. Virieux<sup>2</sup> and S. Operto<sup>1</sup>

<sup>1</sup>Géoazur, Université de Nice Sophia-Antipolis, FRANCE

<sup>2</sup>LGIT, Université Joseph Fourier, FRANCE

1<sup>st</sup> QUEST Workshop

Capo Caccia, Sardinia, 2010 September 19-25

## 1 Introduction

## 2 DG-FEM

- Spatial and time discretizations
- Tetrahedral meshing
- Boundary conditions
- Convergence study
- Computing aspects
- hp-adaptivity

## 3 EUROSEISTEST Verification and Validation Project

- Model description
- Mesh building
- Numerical results

## 4 Conclusions and perspectives

## 1 Introduction

## 2 DG-FEM

- Spatial and time discretizations
- Tetrahedral meshing
- Boundary conditions
- Convergence study
- Computing aspects
- hp-adaptivity

## 3 EUROSEISTEST Verification and Validation Project

- Model description
- Mesh building
- Numerical results

## 4 Conclusions and perspectives

## We investigate the potentials of DG-FEM for 3D seismic modeling

### Advantages

- Common to FEM
  - Arbitrary mesh geometry (fit of complex topographies)
  - Adaptive mesh to physical properties (h-adaptivity)
  - Local method suitable for parallel computing
- Specific to DG-FEM
  - Interpolation order mixing (p-adaptivity)
  - Discontinuous wavefield can be supported (fluid/solid interface)

### Drawbacks

- Computational cost, but...

## We investigate the potentials of DG-FEM for 3D seismic modeling

### Advantages

- Common to FEM
  - Arbitrary mesh geometry (fit of complex topographies)
  - Adaptive mesh to physical properties (h-adaptivity)
  - Local method suitable for parallel computing
- Specific to DG-FEM
  - Interpolation order mixing (p-adaptivity)
  - Discontinuous wavefield can be supported (fluid/solid interface)

### Drawbacks

- Computational cost, but...

**DG-FEM is competitive with other methods when complex topographies or extreme velocity contrasts are considered**

## Characteristics of our approach

- 3D velocity-stress formulation in the time-domain
- Unstructured tetrahedral mesh (more flexible than hexahedral mesh)
- Nodal form of DG-FEM
- Constant physical properties per element
- Favour use of low interpolation orders for fine discretisation
- CPML absorbing boundary condition
- Intensive use of interpolation order mixing
  - Adapt the order according to elements size and medium properties
  - Lower order in the CPMLs to reduce the computational cost
- Centered flux (non-dissipative)

## 1 Introduction

## 2 DG-FEM

- Spatial and time discretizations
- Tetrahedral meshing
- Boundary conditions
- Convergence study
- Computing aspects
- hp-adaptivity

## 3 EUROSEISTEST Verification and Validation Project

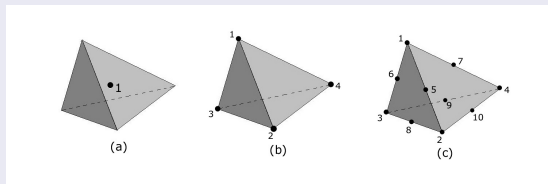
- Model description
- Mesh building
- Numerical results

## 4 Conclusions and perspectives

# DG-FEM - Spatial and time discretizations

## Spatial discretization

- Discretize with non-overlapping and conformal tetrahedra
- Nodal form of DG-FEM (Hesthaven and Warburton, 2008)
- Approximate solution with Lagrangian polynomial basis functions and equidistant nodes



(a)  $P_0$  element with unique DOF. (b)  $P_1$  element with 4 DOF. (c)  $P_2$  element with 10 DOF.

## Time discretization

- Second order explicit leap-frog scheme
- Stability condition for the DG-FEM (Käser et al., 2008) gives  $\Delta t < \frac{1}{2d_i+1} \cdot \min_i \frac{2r_i}{V_{P_i}}$ 
  - $r_i$  is the radius of the sphere inscribed in the element  $i$
  - $V_{P_i}$  the P-wave velocity
  - $d_i$  the interpolation order of the cell
- **The minimum required time step is imposed to all elements**

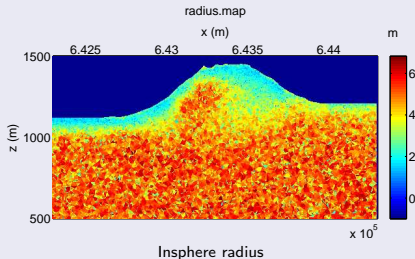
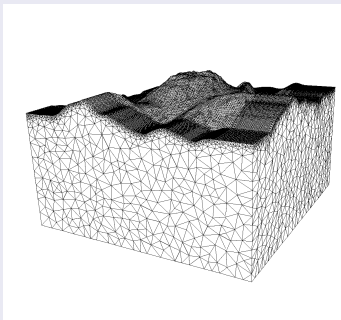


# DG-FEM - Tetrahedral meshing

## Benefits of tetrahedral meshing

- Based on the Delaunay triangulation principle (Delaunay, 1934)
- Great flexibility in terms of design (complex shape) and refinement (local adaptivity)
- Efficient tetrahedral meshers are available (we use TETGEN)

## Example of a complex mesh, the volcano 'La Soufrière'



## Free surface

- Explicit condition by changing locally the flux expression
- Introduce virtual cells which are exactly symmetric to the cells located on the free surface
- Inside these cells, impose identical velocity but opposite stress wavefield

## Absorbing condition

- Convolutional Perfectly Matched Layer (CPML) (Komatitsch and Martin, 2007)
- Unsplit formulation with memory variables
- Improve absorption of waves at grazing incidence
- In the CPML, the damping function is defined in the frequency domain as follows

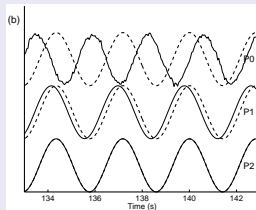
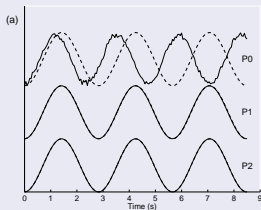
$$s_{\theta} = \kappa_{\theta} + \frac{d_{\theta}}{\alpha_{\theta} + i\omega} \quad \forall \theta \in \{x, y, z\}$$

with the angular frequency  $\omega$  and  $\kappa_{\theta} \geq 1$  and  $\alpha_{\theta} \geq 0$

- If  $\kappa_{\theta} = 1$  and  $\alpha_{\theta} = 0$ , one get the classical PML formulation (Berenger, 1994)

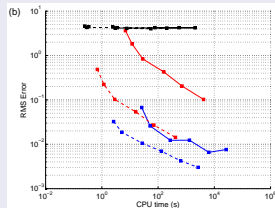
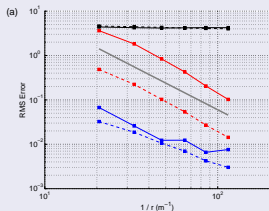
# DG-FEM - Convergence study

## Eigen mode in a cube



Initial conditions + free surfaces = continual monochromatic signals

## Convergence rate

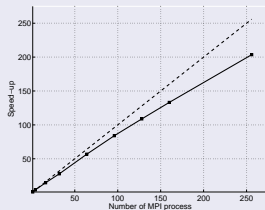
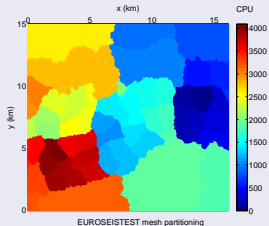


Second order convergence for  $P_1$  (red) or  $P_2$  (blue), but no convergence for  $P_0$  (black)

# DG-FEM - Computing aspects

## Parallelism

- Domain decomposition strategy, one subdomain = one CPU
- MPI communication between subdomains
- Efficient load balancing with mesh partitioning (METIS)
- **Average parallelism efficiency of 80 %**

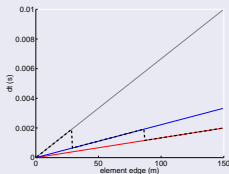


## Possible bottle-neck

- Time step is common for all subdomains
- Dramatic effects of badly shaped elements
- **Mitigate these negative effects with p-adaptivity**

Interpolation order mixing : an efficient mean to mitigate effects of badly shaped tetrahedra

**Downgrade order of badly shaped element = increase time step**



Time step versus the element size for different interpolation orders with  $V_P = 6000$  m/s  
Grey curve :  $P_0$ ; blue curve :  $P_1$ ; red curve :  $P_2$ ; dashed line : interpolation order mixing

## Our 2-step refinement approach

- 1<sup>st</sup> step : Iterative **mesh refinement** (h-adaptivity)
  - based on medium properties and discretization target (3 cells /  $\lambda$  with  $P_2$ )
  - repeated until required discretisation is reached
- 2<sup>nd</sup> step : **adapt the interpolation order** with an **a priori error estimate** (p-adaptivity)

$$\left. \begin{array}{l} P_2 \quad \text{if } \lambda/8 < \text{cell size} \\ P_1 \quad \text{if } \lambda/24 < \text{cell size} \leq \lambda/8 \\ P_0 \quad \text{if } \text{cell size} \leq \lambda/24 \end{array} \right\} \text{heuristic criteria}$$

- 1 Introduction
- 2 DG-FEM
  - Spatial and time discretizations
  - Tetrahedral meshing
  - Boundary conditions
  - Convergence study
  - Computing aspects
  - hp-adaptivity
- 3 EUROSEISTEST Verification and Validation Project**
  - Model description
  - Mesh building
  - Numerical results
- 4 Conclusions and perspectives

## EUROSEISTEST Verification and Validation project

- Organized by CEA, LGIT, University of Thessaloniki and Institute Laue Langevin
- 10 modeling teams (FDM, FEM, SEM, DEM, DG-FEM and PSM)

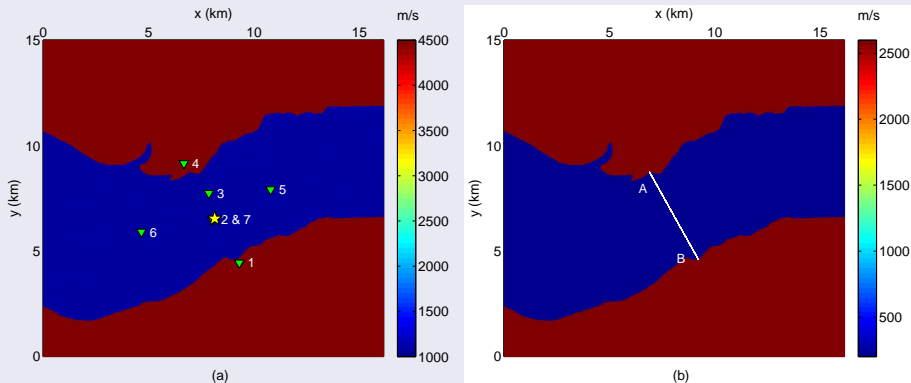
## Model characteristics

- Sedimentary basin 30 km E-NE of Thessaloniki (Northern Greece)
- Low velocity in basin and high velocity bedrock

	P-wave velocity	S-wave velocity	Ratio $V_P / V_S$	Max. depth
Basin	from 1000 to 3027 m/s	from 200 to 848 m/s	from 5.00 to 3.57	411 m
Bedrock	from 4500 to 6144 m/s	from 2600 to 3444 m/s	from 1.73 to 1.78	8 km

- **Ratio Max.  $V_S$  / Min.  $V_S = 17$**
- High Poisson ratio in the basin
- **Thin structures**
- Double-couple source with max. frequency of 4 Hz ( $M_w = 1.3$ )

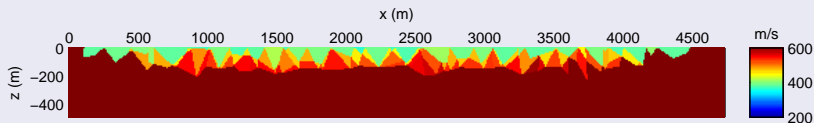
## Velocity model



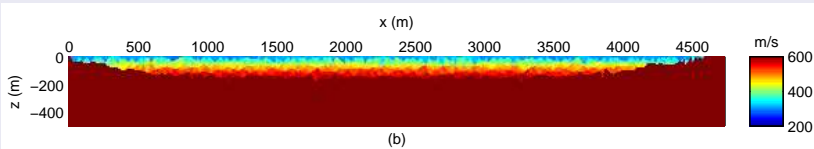
(a) View of the mesh in the  $xy$  at  $z = 0$  m showing the P-wave velocity associated to each cell in the EUROSEISTEST model. The receivers are represented with numbered green triangles and the source epicenter with a yellow star. (b) Same with S-wave velocity associated to each cell. The direction of the cross-section  $AB$  is indicated with a white segment.



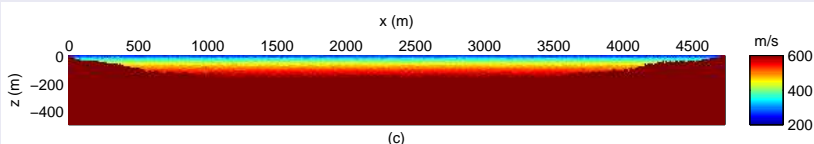
## Iterative mesh refinement (h-adaptivity)



(a)



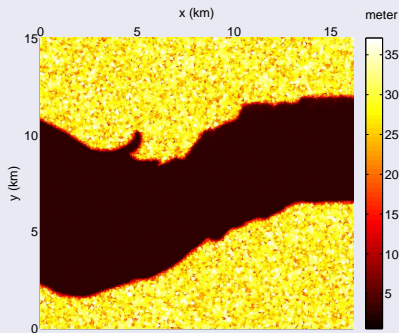
(b)



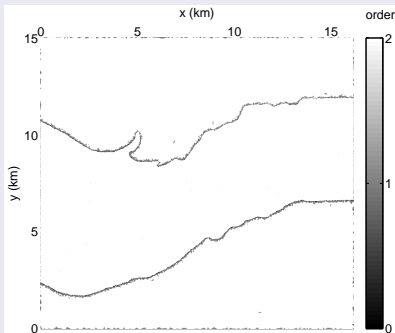
(c)

(a) Cross section  $AB$  of the mesh at the first iteration of the  $h$ -refinement showing the S-wave velocity associated to each cell in the EUROSEISTEST model. (b) Same as (a) at the second iteration of the  $h$ -refinement. (c) Same as (a) at the sixth and last iteration of the  $h$ -refinement.

## Interpolation order mixing (p-adaptivity)



(a)



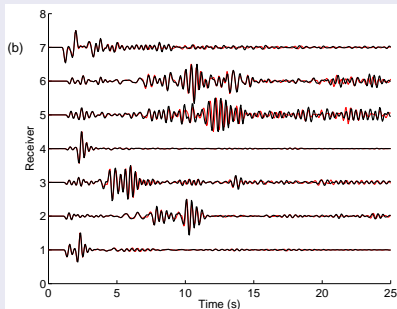
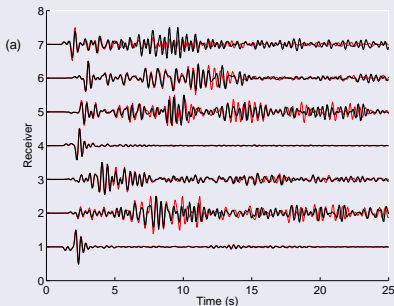
(b)

(a) View of the mesh in the plan  $xy$  at  $z = 0$  m showing the size of the elements (insphere radius) in the EUROSEISTEST model.

(b) Same with interpolation order associated to each cell.  $P_2$  elements are represented in white,  $P_1$  in grey and  $P_0$  in black.

- The basin represents 1 % of the model and contains more than 70 % elements in the mesh
- 65.51 %  $P_2$ , 34.36 %  $P_1$  (with 31.51 % in CPML) and 0.13 %  $P_0$  elements
- **Interpolation order mixing plays an important role at the basin edges**

## Comparison between DG-FEM and SEM

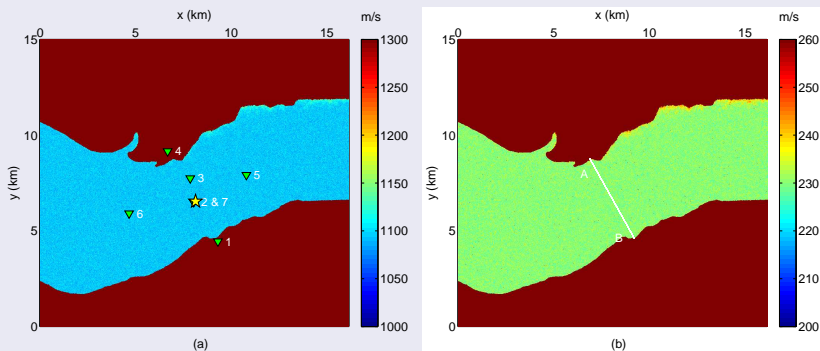


(a) Seismograms of  $v_x$  computed with DG-FEM (black line) and SEM (red line). (b) Same as (a) with  $v_z$ .

- Perfect match between both solutions for receivers in bedrock (1 and 4)
- For other receivers
  - for  $v_z$  very good agreement
  - for  $v_x$  good for short times but misfits are increasing with time

## Model discretization

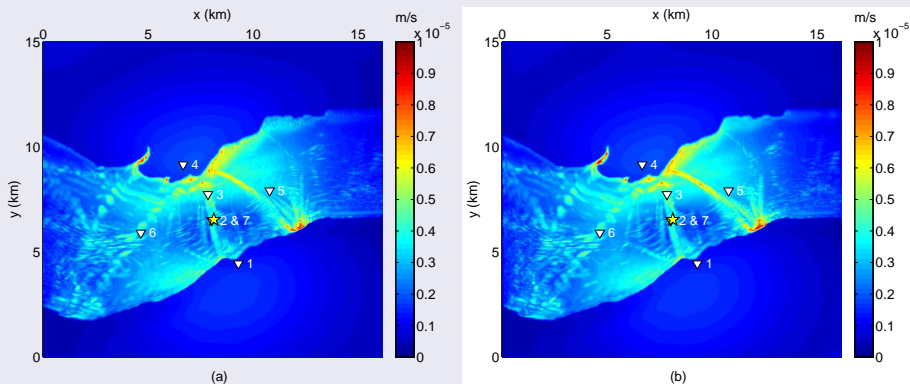
When looking closely at the free surface with a reduced velocity scale...



**Due to constant properties per element, velocities at the free surface are higher than real values ( $V_P = 1000$  m/s and  $V_S = 200$  m/s)**

**⇒ It may be the origins of the misfits at long times**

## Comparison between DG-FEM and SEM



**Excellent agreement of the PGV maps between DG-FEM and SEM**

## Comparison between DG-FEM and SEM

If time permits,  
let's see a little movie of the ground motion...

## Comparison between DG-FEM and SEM

### Mesh statistics

Method	Order	$l_{min}$	$l_{max}$	Nb elements	Nb DOF	Nb unknowns
DG-FEM	$P_2/P_1/P_0$	2.5 m	399.8 m	$16.3 \times 10^6$	$131.6 \times 10^6$	$1.31 \times 10^9$
SEM	$P_4$	20.0 m	908.0 m	$1.4 \times 10^6$	$91.7 \times 10^6$	$0.27 \times 10^9$

### Computation times

Method	Nb time steps	Nb procs	CPU time	Mem.	CPU type
DG-FEM	122 565	144	52h	26 GB	IBM E5420 2.5 Ghz
SEM	75 000	144	7h	25 GB	IBM E5420 2.5 Ghz

- Ratio DG-FEM CPU time / SEM CPU time is 7 (for similar accuracy)
  - Number of unknowns is 4.8 times higher with DG-FEM
  - Number of time steps is 1.6 times higher with DG-FEM
- **In more complex media, DG-FEM should be more competitive...**

- 1 Introduction
- 2 DG-FEM
  - Spatial and time discretizations
  - Tetrahedral meshing
  - Boundary conditions
  - Convergence study
  - Computing aspects
  - hp-adaptivity
- 3 EUROSEISTEST Verification and Validation Project
  - Model description
  - Mesh building
  - Numerical results
- 4 Conclusions and perspectives



## Conclusions

- DG-FEM has great potentials for seismic modeling in highly heterogeneous media
- Designed an effective hp-adaptive scheme (CPU time reduced by one order of magnitude)
- Approach has been validated with the EUROSEISTEST Verification and Validation Project

## Perspectives

- Take into account anisotropy
- Allow for physical properties variation inside elements
  - Explore higher orders in space
  - Explore higher orders in time
- Implement visco-elastic rheologies (Käser et al., 2007)
- Wave propagation in fractured media
- Dynamic rupture (BenJemaa et al., 2007, 2009; de la Puente et al., 2009)
- Application of the method to Full Waveform Inversion (FWI)

- BenJemaa, M., Glinsky-Olivier, N., Cruz-Atienza, V. M., and Virieux, J. (2009). 3D Dynamic rupture simulations by a finite volume method. *Geophys. J. Int.*, 178 :541–560.
- BenJemaa, M., Glinsky-Olivier, N., Cruz-Atienza, V. M., Virieux, J., and Piperno, S. (2007). Dynamic non-planar crack rupture by a finite volume method. *Geophys. J. Int.*, 171 :271–285.
- Berenger, J.-P. (1994). A perfectly matched layer for absorption of electromagnetic waves. *Journal of Computational Physics*, 114 :185–200.
- de la Puente, J., Ampuero, J.-P., and Käser, M. (2009). Dynamic Rupture Modeling on Unstructured Meshes Using a Discontinuous Galerkin Method. *J. Geophys. Res.*, 114 :B10302.
- Delaunay, B. (1934). Sur la sphère vide. *Bul. Acad. Sci. URSS, Class. Sci. Nat.*, pages 793–800.
- Hesthaven, J. S. and Warburton, T. (2008). *Nodal Discontinuous Galerkin Method. Algorithms, Analysis, and Application*. Springer, New York.
- Käser, M., Dumbser, M., de la Puente, J., and Igel, H. (2007). An Arbitrary High Order Discontinuous Galerkin Method for Elastic Waves on Unstructured Meshes III : Viscoelastic Attenuation. *Geophysical Journal International*, 168(1) :224–242.
- Käser, M., Hermann, V., and de la Puente, J. (2008). Quantitative accuracy analysis of the discontinuous Galerkin method for seismic wave propagation. *Geophysical Journal International*, 173(2) :990–999.
- Komatitsch, D. and Martin, R. (2007). An unsplit convolutional perfectly matched layer improved at grazing incidence for the seismic wave equation. *Geophysics*, 72(5) :SM155–SM167.